NEW GLOBAL MEAN DYNAMIC TOPOGRAPHY FROM A GOCE GEOID MODEL, ALTIMETER MEASUREMENTS AND OCEANOGRAPHIC IN-SITU DATA

Rio M-H [(1)], Mulet, S. [(1)], Picot, N. [(2)]

[(1)] *CLS,8-10 rue Hermès 31520 Ramonville Saint-Agne, France, Email:mrio@cls.fr*
[(2)] *CNES,18 avenue Edouard Belin, 31400 Toulouse, France, Email:Nicolas.Picot@cnes.fr*

ABSTRACT

The use of recent GOCE geoid models together with an altimeter Mean Sea Surface significantly improves the estimate of the ocean Mean Dynamic Topography at 100 km resolution compared to the use of previous GRACE geoid models. However, at scales shorter than 100km, the combined effect of geoid omission and commission errors prevents from directly using such models to estimate the ocean MDT and additional information is needed.

In this study, the methodology used by [1] to estimate the CNES-CLS09 MDT is applied to include the shortest scales provided by in-situ measurements of current velocities and dynamic heights and compute a new, high resolution Mean Dynamic Topography for the global ocean.

Improvements over the previous CNES-CLS09 MDT are quantified through comparison to independent in-situ velocities.

1. INTRODUCTION

The accurate knowledge of the ocean Mean Dynamic Topography (MDT) is mandatory for a number of oceanographic applications, including the assimilation of altimeter Sea Level Anomalies into numerical ocean forecasting systems. The ocean MDT is simply the difference between an altimeter Mean Sea Surface (MSS), i.e. the gridded average over a given period of the altimeter measurements of the sea level above a reference ellipsoid, and the geoid height above the same reference ellipsoid. Thanks to the recent dedicated space gravity missions as GRACE and GOCE, the knowledge of the geoid at scales of around 100-150 km has greatly improved in the past years, so that the ocean MDT is now resolved at those scales with centimetre accuracy using this simple approach. However, the true ocean MDT over a given period (classically from 7 to 10 and more years) may contain shorter scales and external information is needed.

To compute higher resolution MDT, a number of methodologies have been developed. The geoid itself can be improved at short scales locally using in-situ gravimetric data or globally using the shortest scales information of the altimetric Mean Sea Surface. On the other hand, the large-scale MDT based on the satellite-only geoid models may be improved thanks to the use of in-situ oceanographic measurements (drifting buoy velocities, dynamic heights from hydrological profiles). This approach was used by [1] to compute the CNES-CLS09 MDT. In this paper, we have used this same approach to compute an improved solution based on updated and upgraded input datasets.

2. DATA AND METHOD

The first step is to compute a large scale first guess of the ocean Mean Dynamic Topography by combining an altimeter Mean Sea Surface (which is the sum of the geoid height and the ocean Mean Dynamic Topography) and a recent geoid model. For that purpose, we have used the CNES-CLS11 Mean Sea Surface [2] together with one of the latest versions of the GOCE geoid delivered by the European Space Agency (ESA) High Processing Facility (HPF), the EGM-DIR R4 model computed by [3].

The raw difference between the two surfaces is polluted by both commission and omission errors on the geoid model and further filtering is required to keep only the spatial scales at which the geoid is known with sufficient, centimetric, accuracy (~125 km, [4]). This is further described in section 3.

To improve the obtained MDT at scales shorter than 125km, synthetic estimates of the mean heights and mean geostrophic velocities are built from in-situ measurements of the ocean state (heights and surface velocities) from which the temporal variability as measured by altimetry is removed. The in-situ measurements dataset consist in hydrological profiles measured by ARGO floats and CTD/XBT casts from the CORA3.2 database as well as SVP-type drifting buoy data for the period 1993-2012. SVP type drifters consist of a surface float connected to a sub-surface 7 meter long holey sock drogue centered at 15m depth. Such a design was thought to minimize the wind slippage so that the drogue drifters follow the currents at 15m depth. In case of drogue loss, the drifter is advected by the surface currents and in addition, is subject to wind slippage. After an anomaly had been evidenced in the drogue loss detection of these drifters ([5], [1]), the estimation of the exact drogue loss time has been recently revisited at the SD-DAC ([6], [7]) for data prior to December 2010. The number of drifter velocities in 4° by 4° boxes is shown on Fig.1 for drogued drifters (top left) and undrogued drifters (top right). We have also used the surface velocity information included in the YOMAHA dataset ([8]) for the period

2000-2013. The surface velocity is deduced from the displacement of ARGO floats at the surface between two dives. The YOMAHA dataset provides the surface velocity information together with an estimate of the surface velocity error. The number of velocities available in 4° by 4° boxes is displayed on the bottom plot of Fig.1
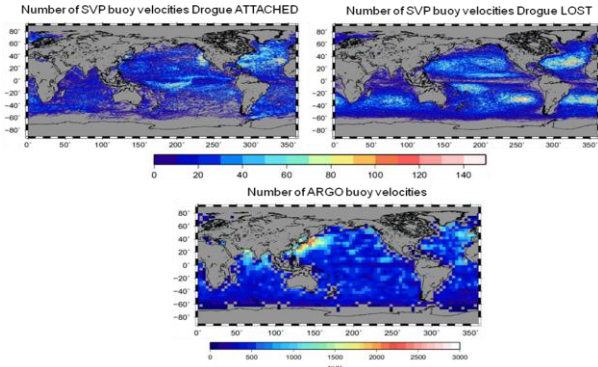

Figure 1: (Top) Number of drogued (left) and undrogued (right) SVP buoy velocities into ¼° boxes. (Bottom) Number of Argo float surface velocities into 4° boxes.

The in-situ data are processed in order to match the altimeter data physical content. In particular, the surface velocities derived from the drifting buoy trajectories are corrected from the Ekman current contribution and the direct wind slippage, that might be quite significant in case of drogue loss. This is described in further details in section 4 for the drifting buoy velocities and section 5 for the hydrological profiles.

The synthetic mean heights and velocities are then used to improve the 125km resolution MDT based on GOCE data through a multivariate objective analysis. A new, high resolution, global MDT (the CNES-CLS13 MDT) is obtained that is validated in section 6.

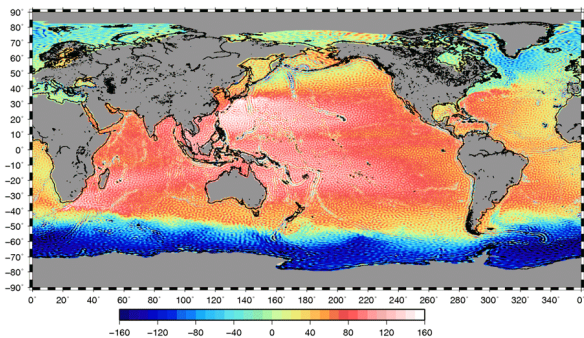## 3. COMPUTATION OF THE FIRST GUESS

Figure 2: Raw difference between the CNES-CLS11 Mean Sea Surface and the EGM-DIR R4 geoid model

The Mean Dynamic Topography First Guess is obtained by filtering the raw difference (Fig.2) between the CNES-CLS11 altimeter Mean Sea Surface [2] and the EGM-DIR R4 GOCE geoid model computed by [3] using 2 years of reprocessed GOCE data together with 7,5 years of GRACE data.

As discussed in [1], isotropic Gaussian filters fail at separating the different error contributions. By removing the strong unrealistic errors in subduction areas due to geoid omission errors, the risk is to oversmooth the strong oceanic realistic gradient, in western boundary currents for instance. Therefore we rather apply an optimal filter. This is done by considering the raw heights from Fig.2 as observations of the MDT, to which an error field is associated, and by mapping these observations using an objective analysis. A first guess is used for the inversion, which is the large scale MDT obtained using a 200km resolution Gaussian filter. Error on the observations is estimated by taking the variance in 1° boxes of the difference between the observations and the MDT from an ocean circulation model. We have used the GLORYS2V1 MDT for that purpose [9]. The correlation lengths used for the inversion have been calculated from the ¼° GLORYS1V1 Mean Dynamic Topography, after the spatial sales greater than 200km have been removed. (The inversion being done on the raw observations minus the 200km resolution large scale first guess).
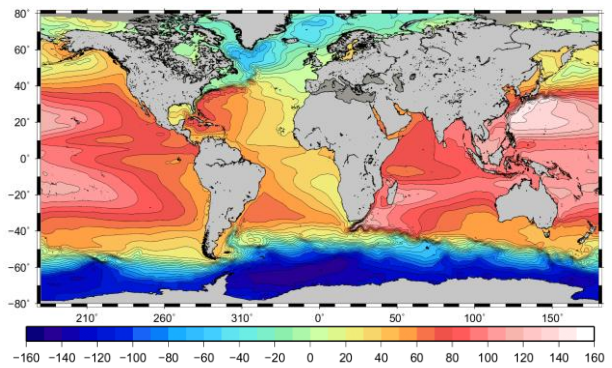

Figure 3: Mean Dynamic Topography obtained by optimal filtering of the raw differences between the CNES-CLS11 MDT and the EGM-DIR R4 GOCE geoid model.

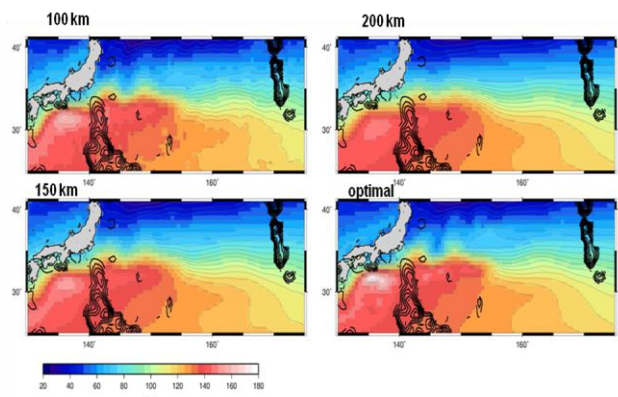We obtain the optimally filtered MDT displayed on Fig.3.

Figure 4: MDT computed from the difference between MSS CNES-CLS11 and EGM-DIR-R4 (top-left) filtered at 100 km, (top-right) filtered at 200 km, (bottom-left) filtered at 300 km and (bottom-right) optimally filtered in the Kuroshio area.

The zoom in the Kuroshio area (Fig.4) illustrates how the optimal filter succeeds in adding realistic short scales to the 200 km resolution mean $\overline{h}$. The optimally filtered MDT resolves sharper gradients than the 100 km filtered MDT (see the Kuroshio current) while reducing noise more efficiently. It filters higher scales (close to 150 km) in areas where prescribed error is high like in the high gravity gradient Izu-Bonin trench.

4. COMPUTATION OF MEAN GEOSTROPHIC VELOCITIES

To compute synthetic mean velocities we have used all in-situ velocities computed from the trajectories of SVP-type drifters and distributed in delayed-time by the Surface Drifter Data Assembly Center (SD-DAC).

In order to compute synthetic estimates of the mean geostrophic surface currents, these velocities have to be processed. First the Ekman component shall be modeled and removed. Then, a 3 days low pass filter is applied to get rid of the other ageostrophic currents (inertial oscillations, stokes drift, tides…). Finally, the geostrophic velocity anomalies derived from multimission altimeter maps of Sea Level Anomalies (SLA) are interpolated along the buoy trajectories and subtracted from the instantaneous geostrophic velocities to end up with an estimate of the mean geostrophic velocities.

4.1. Estimating the Ekman currents at 15m depth

For estimating the Ekman currents at 15m depth, we have considered the SVP-type drifters with the drogue attached (Figure1). The modelization of the Ekman currents is based on the approach described in ([10], [1], [6]):

The Ekman response of the ocean $\vec{u}_{ek}$ to the wind stress forcing $\vec{\tau}$ is written using a 2-parameters (b, θ) formulation:

$$\vec{u}_{ek} = b\vec{\tau}e^{i\theta}$$

(1)

To estimate $\vec{u}_{ek}$, absolute altimetric velocities computed using the AVISO altimetric SLA and the first guess computed in task 1.1 were interpolated along the drifting buoy trajectories available from 1993 to 2012 and subtracted from the buoy velocities. The residual ageostrophic current was further filtered using a 30h to 20 days band pass filter to focus on the frequencies where the coherency between the wind stress and the Ekman currents is maximal [10]. Wind stress values from the ERA INTERIM reanalysis were interpolated

along the buoy trajectories and were also band-pass filtered. Then, the b and θ parameters were estimated by least-square minimization. To take into account the variations in stratification, we fitted the 2 parameters by month and into 4° by 4° boxes. Thus, not only the latitudinal but also the longitudinal variations of the Ekman response to the wind is taken into account. An example is shown for the month of January on the left plots of Fig.5.
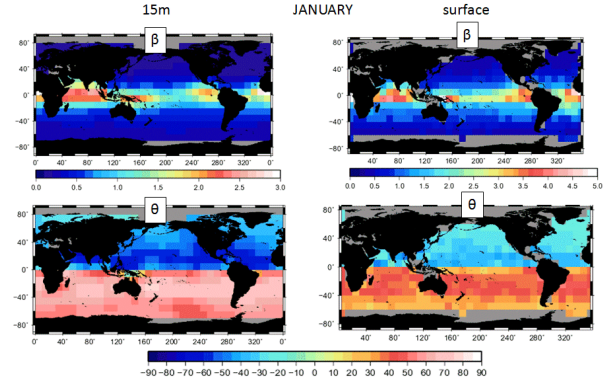

Figure 5: The b and θ parameters of the Ekman model calculated in this study for the month of January from the SVP "drogued-only" drifters (left) and from the Argo floats derived velocities (right).

4.2. Exploitation of the undrogued drifting buoy dataset

The velocity estimates deduced from the trajectories of SVP drifters that have lost their drogue are also calculated at SD-DAC and are available for download. As shown on Fig.1, this represents a very large number of data, so it is worth trying including them in the computation. However, a careful processing must be applied. Indeed, the velocities deduced from undrogued buoy trajectories are the sum of different components:

- The geostrophic velocity, that we want to extract
- The Ekman currents at the surface (and not at 15m depth as for drogued buoys)
- The other ageostrophic components of the current (tides, inertial oscillations, stokes drift)
- The wind slippage, due to the direct action of the wind on the undrogued drifter

The Ekman model calculated in section 4.1 is not applicable since it represents the Ekman currents at 15m depth. Due to the Ekman spiral, the Ekman current at 15m depth may be quite different, both in direction and intensity from the Ekman current at the surface. In section 4.2.1 we present the calculation of a specific surface Ekman model.

Then, in section 4.2.2 we present the wind slippage correction we have applied on the undrogued drifter velocities.

4.2.1 Estimation of the surface Ekman current

In order to estimate the Ekman response of the surface currents to the wind, we have used a database of surface velocities deduced from the trajectories of the Argo floats during the time spent at the ocean surface to transmit their data (usually between 12 and 24 hours).

As for the SVP buoy velocities, we have interpolated and subtracted the altimeter geostrophic velocities (calculated from the altimeter SLA plus the MDT first guess from section 3) at each Argo float velocity date and position. Then we have also interpolated the ERA Interim wind stress values at the Argo float velocity date and position and we have estimated the parameters b and θ from Eq.1 through least square fit. As for the 15m depth Ekman model, we have fitted the b and θ parameters by month and into 4° by 4° boxes. An example is shown for the month of January on the right plots of Fig.5. The structure of the Ekman spiral as represented on Fig.5 is in quite good qualitative agreement with the Ekman theory: The Ekman response at the surface is located at around 40-50° at the right (resp. left) of the wind direction in the northern (resp. southern) hemisphere and the angle then increases with depth.

4.2.2 Estimation of the wind slippage correction

The method used has been fully described in [6]. It consists in removing from each single drifter velocity both the geostrophic and Ekman currents and see how well the residual velocity correlates to local wind. Residual velocities from buoys with the drogue attached should be uncorrelated to the wind while residual velocities from undrogued buoys (for which wind slippage is not negligible anymore) are expected to show a significant correlation to the wind.

A wind slippage contribution is estimated defined as

$$\alpha \vec{W}$$ where α is a slip coefficient and W is the wind vector. The α coefficient is computed so as to further minimize the correlation between the wind and the drifter velocity once the wind slippage has been removed (in addition to the geostrophic component and the Ekman component). For drogued buoys, this wind slippage coefficient was estimated to be less than 0.1% in 10 m/s wind condition by [11].

We have applied the above procedure on the undrogued drifting buoy dataset provided by SD-DAC for the period ranging from January 1993 to September 2012.

The surface Ekman model calculated in section 4.2.1 was then used to estimates the Ekman surface currents $\vec{V}_{Ek}$ along the trajectories of undrogued SVP drifters.

The geostrophic velocity component $\vec{V}_g$ has been calculated from altimetry using the First guess MDT

calculated in section 3 to reference the altimeter SLA.

4.3. Final synthetic mean velocities dataset

The 15m depth Ekman model computed in section 4.1 was used to correct the drogued SVP drifter velocities from the Ekman component. Then, the 3-days low pass filter was applied and the geostrophic velocity anomalies were subtracted. Finally, the resulting mean velocities were averaged into 0.25° by 0.25° boxes. The resulting synthetic mean velocities are shown on Fig.6.

An error was associated to each single synthetic velocity estimate that takes into account:

-   The error on the altimeter velocity anomalies. The error on the zonal (resp. meridional) velocity anomaly is calculated as 30% (resp. 40%) of the zonal (resp. meridional) altimeter velocity variance following [12].
-   Wind slippage. In the case of drogued drifters, the wind slippage is expected to be less than 0.07% of the wind speed in winds lower than 10 m/s [11]. The wind slippage estimation method applied on undrogued SVP drifters (section 4.2.2) was applied on the drogued drifter dataset to estimate a potential residual wind slippage, to be affected as a supplementary error on the dataset.
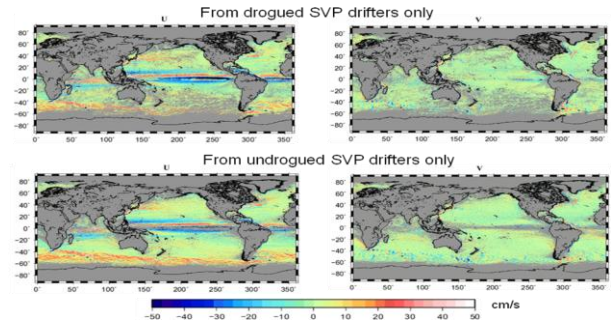

Figure 6: Synthetic mean velocities obtained using (top) the drogue only SVP drifters and (bottom) the undrogued SVP drifter dataset.

Once the undrogued SVP drifter velocities corrected from the surface Ekman currents (4.2.1) and the wind slippage (4.2.2), they were averaged into 0.25° by 0.25° boxes to obtain a dataset of mean synthetic velocities, as displayed on the bottom plots of Fig.6. We see that there is a very good qualitative agreement between the synthetic mean velocities calculated from the drgued and the undrogued drifters. No specific residual bias is obtained in the dataset computed from the undrogued drifters, compared to the dataset from the "drogued" only drifters. This will be confirmed in the next section where different MDTs have been computed using these data and quantitative comparisons to independent velocities performed. Consequently we merged both datastets into a single dataset for the final MDT computation.

5. COMPUTATION OF MEAN HEIGHTS

To calculate the mean synthetic height dataset, the temperature and salinity profiles measured by ARGO floats and CTD casts are first used to compute dynamic heights hdyn/Pref(t,x,y) relative to the profile's reference depth Pref. These dynamic heights reflect the variations of the sea level due to change in density occuring from the surface to the reference level. We first extract from this dynamic height the temporal variability as taken from the steric component of the altimeter Sea Level Anomalies. The steric component is obtained by applying to the altimeter SLA a regression coefficient calculated from an historical collocated dataset of SLA and dynamic height anomalies [13]. This regression coefficient depends both on the profile's reference depth and on its geographical location: For a given reference depth, the regression coefficient decreases from the tropical band (where it is closer to 1) to high latitudes. Furthermore, for a given geographical location, the regression coefficient increases with increasing reference depth.

For each reference depth, mean synthetic dynamic heights are then computed into 0.25° boxes and the scales shorter than 125km (the spatial resolution of the GOCE based first guess) are extracted and added to the first guess to obtain the mean synthetic height dataset (Fig.7). Compared to the full Mean Dynamic Topography signal, the obtained mean synthetic heights miss the barotropic scales shorter than 125km and the contribution from the deep (i.e. deeper than the reference depth) baroclinic scales shorter than 125km.

An error is associated to the mean synthetic heights calculated as the quadratic sum of the first guess error and the variability, computed in 0.25° boxes, of the synthetic mean dynamic heights.
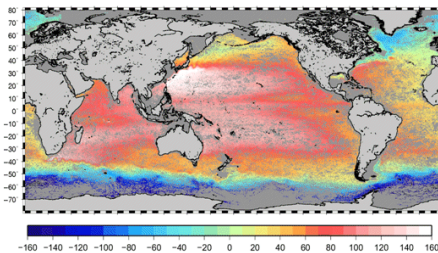

Figure 7: mean synthetic heights

6. RESULT: THE CNES-CLS13 MDT

The different synthetic mean velocities and heights calculated in sections 4 and 5 were used to improve the first guess calculated in section 3 through a remove-restore technique: the first guess estimate is first removed from the synthetic observations and an objective analysis is performed on the residual heights and velocities. Then, the first guess is added back to the estimated field. The input data needed for the inversion are the observations and associated errors, and most importantly the apriori statistics of the MDT field [1]. This is given by the variance and correlation scales obtained as for the first guess computation using the GLORYS2V1 MDT as a-priori.

6.1 First Inversion tests: « DROG ON » dataset versus « DROG OFF » dataset

In order to check the reliability of using the undrogued drifter velocities for the CNES-CLS13 MDT computation, we first started with calculating MDT solutions using separately the "DROG ON" (section 4.1) and the "DROG OFF" (section 4.2) synthetic mean velocity dataset. The global RMS difference between the two obtained MDT is around 1 cm.

We used the Argo float surface velocities to perform quantitative comparison between the two solutions. Synthetic mean geostrophic velocities were computed from the Argo float surface velocities by removing the Ekman surface currents and the altimeter geostrophic velocity anomaly. RMS differences were then calculated for both components of the velocity between the MDT solutions and the Argo float mean velocities. For both solutions ("DROG ON" or "DROG OFF"), the obtained RMS differences are very close (around 45% of the Argo float velocity variance for the zonal component, and around 53% for the meridional component). This result confirmed the validity of the "DROG OFF" dataset for the CNES-CLS13 MDT computation. the use of the full velocity dataset to compute the MDT leads to increased agreement to the independent Argo mean synthetic velocities compared to the "DROG ON" and "DROG OFF" solutions (values of 44.6% and 52.4% were obtained for the zonal and meridional component respectively).

Finally, we have merged all available velocity estimates to produce an unique dataset of synthetic mean velocities from SVP drogued, undrogued drifters (including the SVP drifters released in the framewotk of the Keops campaign) and the Argo floats. This final dataset was used together with the synthetic mean heights to compute the CNES-CLS13 MDT. The obtained solution is shown on Fig.8, and the associated mean geostrophic velocities on the bottom plot of Fig.9.
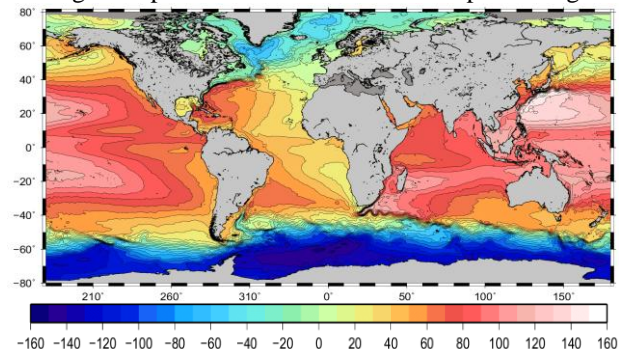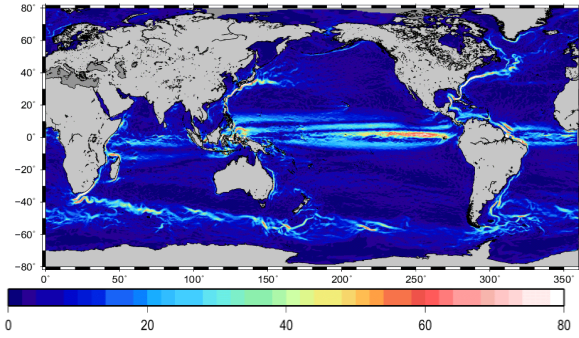
Figure 8: The CNES-CLS13 MDT (m)

Figure 9: The CNES-CLS13 mean geostrophic current speeds (cm/s)

7. VALIDATION

We have performed quantitative comparisons with other existing MDT solutions: the first guess computed in section 3, the DNSC08 MDT [14] based on the filtered difference between a MSS and a combined geoid model, the MDT from [15] based on GRACE and drifters, as well as the MDT from the GLORYS2V1 model reanalysis. The MDT differences are displayed on Fig.10 and the main statistics (mean and RMS of the differences) are given in Tab.1.
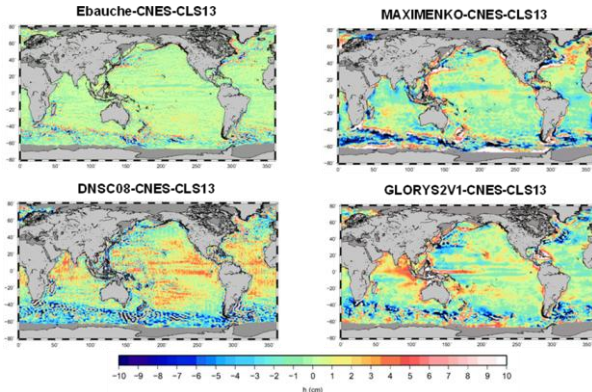

Figure 10 : Differences between the CNES-CLS13 MDT and a- the first guess used in this study; b- the Maximenko et al (2009) MDT; c- the DNSC MDT and d- the GLORYS2V1 MDT

	CNES-CLS09	GLORYS	Max. 2009	DNSC	First Guess
Diff mean (cm)	0.2	43.5	44.2	3.0	-0.01
Diff RMS (cm)	3.5	3.4	5.1	4.4	1.9

Table 1: Mean and Root Mean Square differences between the CNES-CLS13 MDT and different existing MDT solutions

Then, to enable quantitative comparison, we have used

independent measurements of the ocean surface currents provided by SVP-type drifters processed in near-real time and distributed by the Coriolis datacenter for the period ranging from September 2012 to September 2013. The global ocean is rather well sampled so that our comparison results are representative of all regions. This near real-time drifter data have been processed like the delayed-time drifters to correct for the Ekman currents, the potential wind slippage, the residual ageostrophic currents, and the time dependent geostrophic anomaly. We therefore end up with an independent dataset of synthetic mean velocities. In Tab.2, we have displayed the statistical comparison results between these independent mean geostrophic velocities and the mean geostrophic velocities derived from the different MDT solutions listed above.

	MDT-CNES-CLS13	MDT CNES-CLS09	MDT GLORYS2V1	MDT MAX08	MDT GOCE (First Guess)
RMS U	42.17	43.89	44.95	43.52	44.31
RMS V	46.48	47.23	51.49	48.09	49.54

Table 2: RMS differences (expressed in % of drifter velocity variance) between the mean velocities from the different MDT solutions and independent synthetic mean velocities computed using the real-time SVP velocity dataset distributed by the Coriolis datacenter.

Results are expressed in percentage of the independent drifter velocity variance. The RMS differences obtained for both components of the velocity are reduced when using the new CNES-CLS13 MDT compared to the other existing solutions.

8. CONCLUSION

A new global Mean Dynamic Topography has been computed, called the CNES-CLS13 MDT, that beneficiated from the very high accuracy of the last geoid models based on GRACE and 2 years of reprocessed GOCE data. These new data have allowed us to obtain a MDT first guess at around 125km scale with unprecedented accuracy. For the computation of the CNES-CLS09 MDT, the first guess, based on a GRACE model, was resolving scales of around 400km. In addition, an extensive work has been done for the use of current velocities derived from the trajectories of drifting buoys. This work has made possible to include for this MDT computation not only the buoy velocities from SVP-type drifters with the drogue attached, but also the velocities from the buoys having lost their drogued (and being hence advected at the surface both by the ocean currents and the wind) and the surface velocities derived from the trajectories of Argo floats.

Also, Temperature and Salinity profiles from the CORA3.2 database have been processed to compute

synthetic observations of the Mean Dynamic Topography. Together with the synthetic velocity dataset, they have then been used to improve the 125km resolution GOCE based first guess and compute the CNES-CLS13 MDT on a ¼° resolution grid. The CNES-CLS13 MDT was finally shown to give better comparison results to independent velocity observations than other existing MDT solutions.

10. REFERENCES

1. Rio, M. H., S. Guinehut, and G. Larnicol (2011), New CNES-CLS09 global mean dynamic topography computed from the combination of GRACE data, altimetry, and in situ measurements, J. Geophys. Res., 116, C07018, doi:10.1029/2010JC006505.

2. Schaeffer P., Y. Faugere, J. F. Legeais, A. Ollivier, T. Guinle, N. Picot (2012), The CNES CLS11 Global Mean Sea Surface Computed from 16 Years of Satellite Altimeter Data. Marine Geodesy, 2012, Special Issue, Jason-2, Vol.35.

3. Bruinsma, S. L., C. Förste, O. Abrikosov, J.-C. Marty, M.-H. Rio, S. Mulet, and S. Bonvalot (2013), The new ESA satellite-only gravity field model via the direct approach, Geophys. Res. Lett., 40, doi:10.1002/grl.50716

4. Mulet S., M.-H. Rio et S. Bruinsma (2012). Accuracy of the preliminary GOCE GEOID models from an oceanographic perspective. Marine Geodesy, 35:314–336, 2012 DOI: 10.1080/01490419.2012.718230

5. Grodsky, S. A., R. Lumpkin, and J. A. Carton (2011), Spurious trends in global surface drifter currents, Geophys. Res. Lett., 38, L10606, doi:10.1029/2011GL047393

6. Rio, M-H, 2012: Use of altimeter and wind data to detect the anomalous loss of SVP-type drifter's drogue. Journal of Atmospheric and Oceanic Technology DOI:10.1175/JTECH-D-12-00008.1

7. Rick Lumpkin; Semyon A. Grodsky; Luca Centurioni; Marie-Helene Rio; James A. Carton; Dongkyu Lee, Removing spurious low-frequency variability in drifter velocities, JTECH-D-12-00139

8. Konstantin V. Lebedev, Hiroshi Yoshinari, Nikolai A. Maximenko, and Peter W. Hacker, 2007: YoMaHa'07: Velocity data assessed from trajectories of Argo floats at parking level and at the sea surface, IPRC Technical Note No. 4(2), June 12, 2007.

9. Ferry N., L. Parent, G. Garric, C. Bricaud, C.-E. Testut, O. Le Galloudec, J.-M. Lellouche, M. Drévillon, E. Greiner, B. Barnier, J.-M. Molines, N. Jourdain, S. Guinehut, C. Cabanes et L. Zawadzki (2012). Reanalysis of the Altimetric Era (1993-2009) at Meso Scale. Mercator Ocean Quarterly Newsletter, 44.

10. Rio, M.-H. and F. Hernandez, 2003: "High-frequency response of wind-driven currents measured by drifting buoys and altimetry over the world ocean." Journal of Geophysical Research 108(C8): 3283-3301

11. Niiler, P. P., R. Davis, and H. White (1987), Water following characteristics of a mixed layer drifter, Deep Sea Res., Part A, 34, 1867–1881, doi:10.1016/0198-0149(87)90060-4.

12. Le Traon, P.Y. and G. Dibarboure, 2002. Velocity mapping capabilities of present and future altimeter missions: the role of high frequency signals. J. Atm. Ocean Tech., 19, 2077-2088.

13. Guinehut, S., P.Y. Le Traon, and G. Larnicol (2006), What can we learn from global altimetry/hydrography comparisons?, Geophys. Res. Lett., 33, L10604, doi:10.1029/2005GL025551.

14. Andersen, O. B., and P. Knudsen (2009), DNSC08 mean sea surface and mean dynamic topography models, J. Geophys. Res., 114, C11001, doi:10.1029/2008JC005179

15. Maximenko, N., P. Niiler, M-H. Rio, O. Melnichenko, L. Centurioni, D. Chambers, V. Zlotnicki and B. Galperin, 2009: Mean Dynamic Topography of the ocean derived from satellite and drifting buoy data using three different techniques. Journal of Atmospheric and Oceanic Technology. DOI 10.1175/2009JTECHO672.1.